POAC'23
Glasgow, United Kingdom

Proceedings of the 27th International Conference on
Port and Ocean Engineering under Arctic Conditions
12-16 June 2023, Glasgow, United Kingdom

Physical and mechanical properties of brash ice in Luleå Harbour

Vasiola Zhaka[1], Robert Bridges[2], Kaj Riska[3], Jonny Nilimaa[1], Andrzej Cwirzen[1]

[1]Luleå University of Technology, 97187 Luleå, Sweden;

[2]TotalEnergies SE, Paris, France;

[3]Formerly TOTAL SA, France

ABSTRACT

Brash ice forms when vessels navigate in level ice breaking it, and subsequently along the same track breaking the partly or fully consolidated broken ice field. The formation and growth of brash ice can be rapid and present a hazard for shipping operations, often requiring icebreaker assistance. Compared to other deformed ice structures such as pressure ridges, the physical and mechanical properties of the brash ice formed in heavily navigated harbours or ship channels have not been studied much. In the current study, individual brash ice pieces were sampled from two different harbours in Luleå, Sweden, in March 2020 and March 2021. The brash ice piece size distribution, the compressive strength of individual ice pieces, density, microporosity, and microstructure were measured. The brash ice piece size followed a three-parameter log-normal distribution. The brash ice samples collected in the first year (2020) had a microstructure similar to level ice while the ice pieces collected in the second year (2021) had a mixed microstructure (columnar and granular) similar to deformed ice. For an increase in strain rates from 10^{-5} s^{-1} to 10^{-3} s^{-1}, the maximum strength increased when the brash ice samples were exposed to cyclic loading. The maximum strength was not significantly different between the different locations.

KEYWORDS: Brash ice, piece size distribution; strength; cyclic loading; microstructure.

1. INTRODUCTION

On the Swedish coast, in the Bay of Bothnia, fast ice forms in November and breaks up in April every winter. The level ice thickness is typically about 0.5 m, but in very cold winters the fast ice thickness may reach up to 0.8 m (Sankvist,1986). Navigation occurs mainly in the same ship tracks, which are maintained daily by icebreakers operating in this region. Icebreakers and ice-breaking tugs escort merchant vessels in heavy brash ice conditions in ship tracks and assist them also when manoeuvring in harbours.

The repeated freezing and breaking cycles made by the ships continuously transform the shape and size of the brash ice pieces. The pieces are rounder and smaller in size compared to other deformed ice features e.g., ice rubble and ridges. The brash ice piece size and shape depend on the strength of the consolidated brash ice layer and vessel speed (Greisman, 1981; Sandkvist, 1982; Ettema and Huang, 1990). Between two ship passages, the brash ice pieces freeze together at the water surface or in the contact surface. This freezing between two ice pieces can be initially driven by the heat stored in the ice pieces and subsequently can form from atmospheric cooling (Høyland and Liferov, 2005; Boroojerdi et al., 2020). The further consolidation significantly increases the vessel's resistance in brash ice channels (Kitazawa and Ettema, 1985). The frequent freezing-breaking cycles affect the ice crystal orientation (microstructure), density, porosity, and strength of the ice. The microstructure of the naturally formed brash ice is no longer purely granular or columnar ice, but mostly randomly oriented broken and compressed columnar crystals mixed with granular snow ice (Zhaka, et. al. 2020).

The main objective of this study is to investigate the properties of brash ice formed in ports. The physical and mechanical properties of the brash ice formed in two different harbours in Luleå, Sweden, were observed and measured. The results obtained give insight into piece size distribution, density, microporosity, microstructure, and the strength of the individual brash ice pieces. The current results can be used in ship resistance modelling or in optimizing ice management strategies in ports.

2. FIELD STUDY

The brash ice pieces were collected from two different harbours in Luleå, Sweden, respectively on 04-03-2020 at the icebreaker quay (Isbrytarehamnen), where icebreakers Frej, Oden, Atle and Ymer are based, and 12-03-2021 in Luleå harbour (Strömören), a quay for port tugs such as Vilja and Viscaria. The harbour locations are illustrated in Figure 1 and are hereafter addressed as the first and second harbour, Icebreaker harbour and Luleå harbour or the first and second year.

The frequency of navigation in both harbours was different. The first harbour was visited about once a week, while the second harbour was visited daily. In the first year (2020), the ice was broken by an icebreaker before the sampling, while in the second year (2021), the brash ice was broken by a port ice-breaking tug nine hours before the sampling.

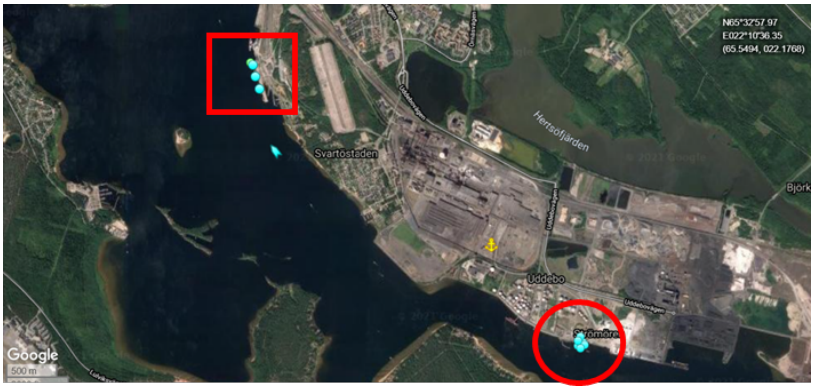

Figure 1. The location of the Icebreaker harbour (red square) where brash ice pieces were sampled in 2020, and Luleå harbour (red circle) where brash ice pieces were sampled in 2021.

3. BRASH ICE SAMPLING

The brash ice conditions for both years are illustrated in Figure 2. The brash ice was collected with a crane and stored in plastic containers for transportation to the cold laboratory of Luleå University of Technology (LTU). The transportation was conducted with an open truck. In 2020, the air temperature was around -15^{O}C, and in 2021, the air temperature was around -5^{O}C. The temperature of the ice pieces in the first year varied from -0.5^{O}C to -2.5^{O}C and in the second year varied between -0.3^{O}C and -1^{O}C. Simultaneously, brash ice pieces were collected and placed in a rubber membrane that was used to test the shear behaviour of brash ice under cyclic loading. These results were discussed in the study by Patil et. al. (2022).

In the first year, 12 brash ice pieces were stored in a freezing box until further laboratory investigations were conducted. The temperature of the freezing box was kept constant at -20^{O}C. In the second year, 169 brash ice pieces were brought to LTU, where the sizes and weights of the individual brash ice pieces were measured, with 13 ice pieces stored in the freezing boxes for further laboratory measurements.

Figure 2. The sampling area; a) Icebreaker harbour; b) Luleå Harbour.

3.1 Sample Preparation and Laboratory Tests

The brash ice pieces collected in the first year were processed in the freezing room during June 2020, while the brash ice blocks sampled in the second year were processed in May 2021. In the first year, the brash ice piece sizes were measured, and cylinders of ice were produced with

a drilling core that has an inner diameter of 70 mm. In total 8 samples with a height between 140 and 170 mm were used to measure the unconfined uniaxial compressive strength at a strain rate equal to 10^{-4} s^{-1}. During sample preparation, the air temperature in the freezing room was between -5 and -10°C. The dimensions and weight of the cylindrical cores were used to determine the density and microporosity of the brash ice assuming zero salinity. In addition, the microstructure of thin ice sections (2-10 mm thick) was observed under cross-polarized light.

The same procedure was followed for the brash ice samples collected in the second year when 17 cylinders were tested under uniaxial compression. Eight samples were compressed under a strain rate of 10^{-4} s^{-1}, and six samples were compressed under a strain rate of 10^{-3} s^{-1}. To better understand the brash ice behaviour under increasing strain rates, as brash ice in harbours and channels may be exposed to different navigation speeds, cyclic loading was applied in three samples. The cyclic loading procedure consisted of the initial compression of samples under a strain rate equal to 10^{-5} s^{-1} and when reaching the first load peak, the sample was compressed with a strain rate equal to 10^{-4} s^{-1}. When the 2nd load peak was reached the strain rate was increased to $10^{-3}s^{-1}$ which gave a third load peak. Examples from the sample preparation and test procedure are illustrated in Fig. 3.

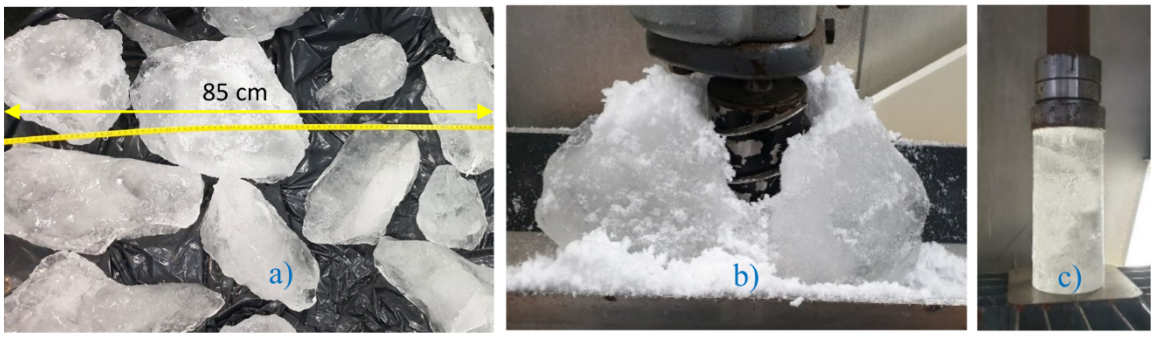

Figure 3. a) An example of the brash ice blocks collected in the second harbour. The yellow arrow and measuring tape are 85 cm long. b) coring a cylindric sample; c) an example of the ice cylinder before being tested in compression.

4. RESULTS AND DISCUSSION

The piece size distribution, microstructure, and strength of the brash ice pieces are presented and discussed.

4.1 Piece size distribution

The three dimensions (length, width, and height) of 12 and 169 brash ice pieces were measured in the first and second years. The descriptive statistics for the brash ice blocks sampled in both harbours are summarised in Table 1. The brash ice piece size dimensions were limited to the sizes of the pieces that could be collected by the crane (about 1 m). The brash ice pieces that were investigated in the first year had maximum sizes that varied between 23 and 52 cm, and 7 to 87 cm in the second year. The ‘average piece size’ used here is the average of the length, breadth and height of each brash ice piece measured. From the 12 different distributions tested, a three-parameter lognormal distribution describes thPiecee brash ice size distribution collected

in the second harbour best, see Figure 4.

Earlier studies have also observed a lognormal distribution (Bonath et. al., 2019b). The number of ice pieces collected in the first year was not sufficient for a distribution fit. The average brash ice piece sizes (PS_{avg}) were plotted against their measured mass (m_i in kg), see Fig. 5a. A good fit for this correlation is the power function:

$$PS_{AVG} = 17.5 m_i^{0.525} [cm] \quad (1)$$

The average piece size between the two years cannot be statistically compared due to the difference in the number of pieces collected and measured. In the first year, the brash ice consisted of big ice floes, while in the second year, the harbour was filled with smaller brash ice pieces. In addition, the ice pieces present in the second harbour looked rounder in shape compared to the ice floes in the first harbour. The average length/height ratio was equal to 2.2 and 2.0 for the brash ice blocks sampled in 2020 and 2021, respectively. The length and height are the largest and smallest dimension of each brash ice piece.

To investigate the piece shape, the sphericity of the brash ice pieces is defined here as the ratio between the mass of the actual brash ice pieces and the mass of a perfect ice sphere. The mass of the perfect ice sphere was calculated from the volume-density function. The volume of the perfect ice sphere was determined firstly by considering the length of the brash ice pieces equal to the sphere's diameter, and secondly using the average piece size instead of the length. The latest assumption is expected to increase the sphericity.

The average density (900 kg m^{-3}) measured from the brash ice cylindric samples was used to determine the mass of the sphere. The ratio between the actual mass and the mass of a perfect sphere (diameter = average piece size) is plotted against the average piece size of brash ice, see Fig. 5. If the brash ice pieces were spheres, the mass ratio would be equal to one. For the harbour brash ice pieces, with an average piece size between 5 and 66.7 cm, the mass ratio varied between 0.037 and 0.219 when the sphere's diameter was considered equal to the length of the individual brash ice pieces. When the sphere's diameter was considered equal to the average piece size, the sphericity doubled and was 0.085 to 0.52. A study that proposed a shape concept for brash ice pieces estimated the sphericity factors between 0.1 and 0.5 for model brash ice, with the highest probability being equal to 0.2 (Matala and Gong, 2021). While for the harbour brash ice, the most common ratio was around 0.4 to 0.5 for average brash ice pieces between 5 to 10 cm.

Table 1. A Summary of the statistical values of brash ice pieces measured in the two different harbours, including the average piece size considering all three dimensions in cm (Mean), the standard deviation (Stdev), the Median, minimum and maximum piece sizes in cm. L/H is the length/height ratio.

Year	Count	Mean (cm)	Stdev	Median	Min (cm)	Max (cm)	L/H
2020	12	24.7	6.6	23	18	41.7	2.2
2021	169	13.7	10.8	10.0	5.0	66.7	2.0

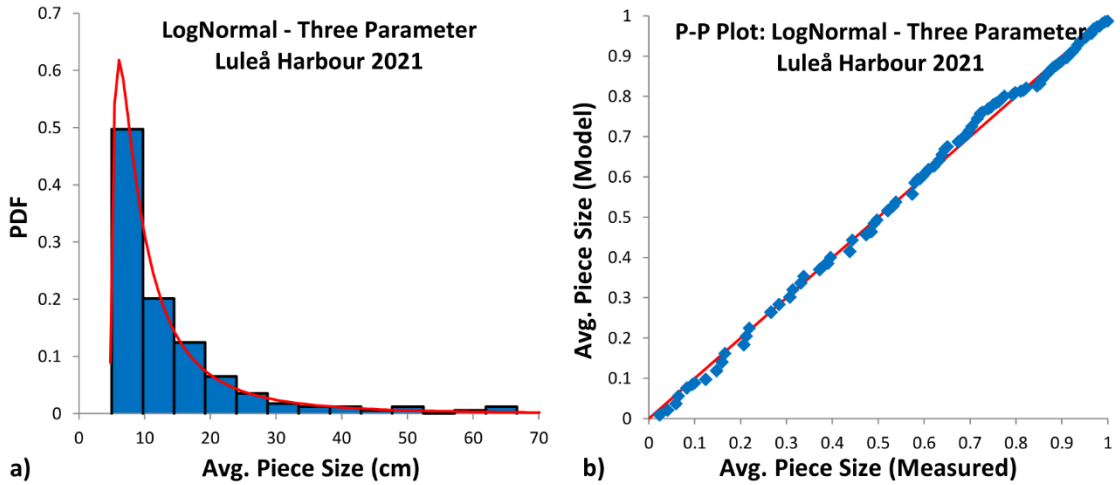

Figure 4. a) The histograms and the probability density function (PDF) line of the three-parameter lognormal distribution for brash ice average piece sizes. b) The P-P (probability-probability) plot of the three-parameter lognormal distribution for the average brash ice piece size.

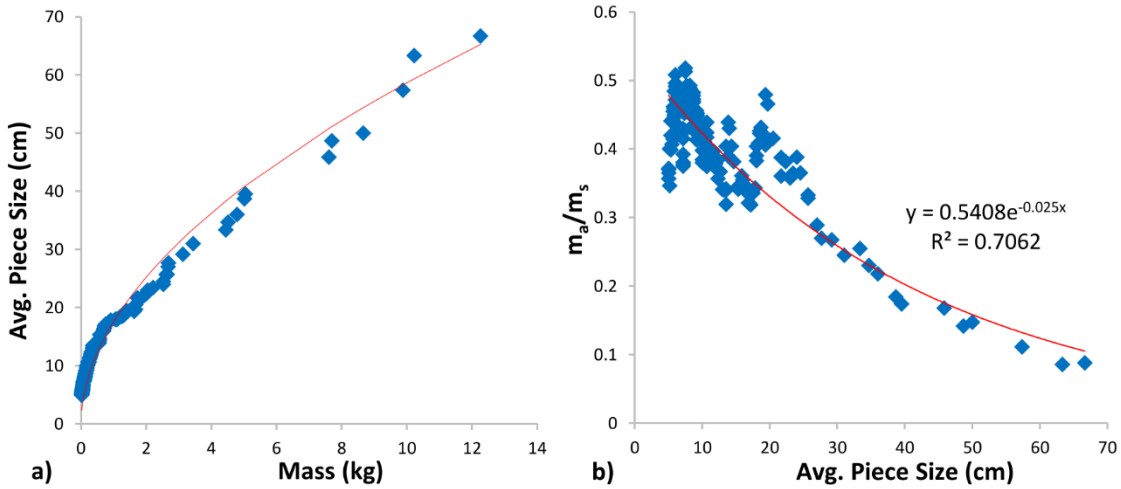

Figure 5. a) Average piece size of the brash ice plotted against the mass of individual brash ice pieces. The red line follows Eqn. 1. b) The ratio between the actual mass (m_a) of individual brash ice pieces and the mass of a sphere (m_s) with a diameter equal to the measured length of the brash ice pieces plotted against the brash ice piece size.

4.2 Microstructure

The brash ice collected in the first harbour (2020) had mainly columnar crystals with c-axes oriented both vertically and horizontally, see Figure 6. Mixed columnar ice with snow ice and randomly oriented crystals were observed in small amounts. Assuming that the level ice layer is mostly composed of columnar ice under a granular ice layer (snow ice) then the microstructure of brash ice from the first harbour was similar to the parental ice sheet (Eicken, 2003), which indicates that the harbour was not frequently navigated.

The brash ice pieces sampled in Luleå Harbour in 2021 consisted of fractions of columnar ice randomly oriented mixed with granular snow ice. This microstructure was similar to the microstructure of deformed ice (Bonath et al., 2019a). The microstructure and the brash ice piece sizes and shapes observed (rounder and smaller than the first harbour) indicate that the second harbour was more frequently navigated.

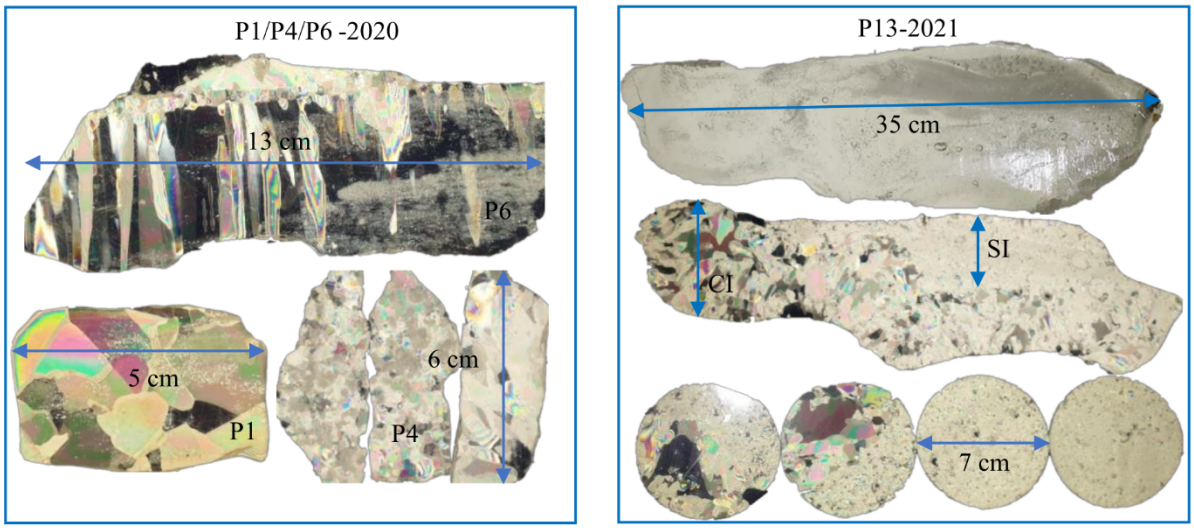

Figure 6. The microstructure of brash ice pieces collected from the Icebreaker harbour in the first year (left), and from the Luleå harbour in the second year (right). The blue arrow shows the scale in cm while, P1 for example stands for brash ice Piece 1. SI and CI are snow ice and columnar ice, respectively.

4.3 Brash ice strength

The summary of test results, including the average maximum strengths, average densities, and porosities are given in Table 2. All the cylinders cored from the brash ice collected from both harbours showed ductile behaviour for a strain rate equal to 10^{-4} s^{-1}. The cylinders sampled from the second harbour showed brittle behaviour for a higher strain rate of 10^{-3} s^{-1}. The same behaviour was also reported earlier for sea ice (Timco and Frederking,1990; Moslet, 2007; Zhaka et. al., 2020).

The average strength of samples cored at different strain rates and different years is illustrated in Fig. 7a. The compressive strength values were similar to values earlier reported for sea ice (Moslet, 2007). The compressive strength of the ice slightly increased and thereafter decreased for strain rates from 10^{-3} to 10^{-4} and 10^{-5} s^{-1}. The average compressive strength for brash ice sampled in both harbours under strain rate 10^{-4} s^{-1} was similar but the standard deviation was higher for the samples from the first harbour.

The average compressive strength of the individual ice blocks sampled in both harbours was considerably lower, compared to the previously investigated strength of the refrozen brash ice (RBI) sampled in a fully consolidated ship channel in Marjaniemi Harbour in Bay of Bothnia, Finland (Zhaka. et. al., 2020), see Fig. 7b. For example, the average strength of brash ice sampled in the harbours was 65% lower for a strain rate of 10^{-3} s^{-1} and 32% lower for a strain

rate of 10^{-4} s^{-1}. The sample preparation was carried out in the same laboratory and the testing procedure was similar for both harbour brash ice and brash ice sampled in the refrozen ship channel in Finland. The temperature of the ice samples during the test may be the cause of the strength difference. The average temperature of the ice cylinders from the first harbour varied between -2 and -4°C with an average value of -2.9°C. The temperature of harbour ice cylinders tested in 2021 varied between -2.5 to -12 with an average of -6.7°C. The temperature of the RBI tested under a strain rate of 10^{-4} s^{-1} was between -9 and -13°C with an average value of -11°C, while the RBI samples compressed with a strain rate of 10^{-3} s^{-1} had an average temperature of -10.4°C. Another reason for this significant difference in compressive strength could be the longer exposure of the refrozen brash ice to freezing air temperatures, which may increase the bond strength of the consolidated layer (Boroojerdi et. al., 2020). On the other hand, the harbour's brash ice was exposed to daily breaking events that continuously mix the ice with the warmer water.

In addition, the average compressive strength of the brash ice sampled in the harbours is comparable to the strength of level ice measured in different locations in the Gulf of Bothnia, (Fransson et. al., 2008). The compressive strength of level ice was reported between 1 and 7 MPa. Strengths below 2 MPa were observed due to premature cracking. Another study reported the compressive strength of the model brash for a consolidation time of 20 to 50 hours, which varied between 0.6 and 1.6 MPa (Bridges et. al., 2019). From Table 2, the average strength is seen to increase when decreasing average porosity, and the same trend was earlier reported for undeformed and deformed ice (Moslet, 2007; Shafrova and Høyland, 2008; Bonath et. al., 2019).

Table 2. Summary of compression strength test results from brash ice pieces sampled from the two different harbours in Luleå.

Year	No. Cores	Strain rate (s^{-1})	σ_{avg} (MPa)	Std (σ_{avg})	ρ_{avg} (kg m^{-3})	P (%)
2020	8	0.0001	2.95	0.70	906.5	1.2
2021	6	0.001	2.22	0.30	895.6	2.4
	8	0.0001	2.82	0.31	902.9	1.6
	3	0.00001	2.16	0.14	900.8	1.9

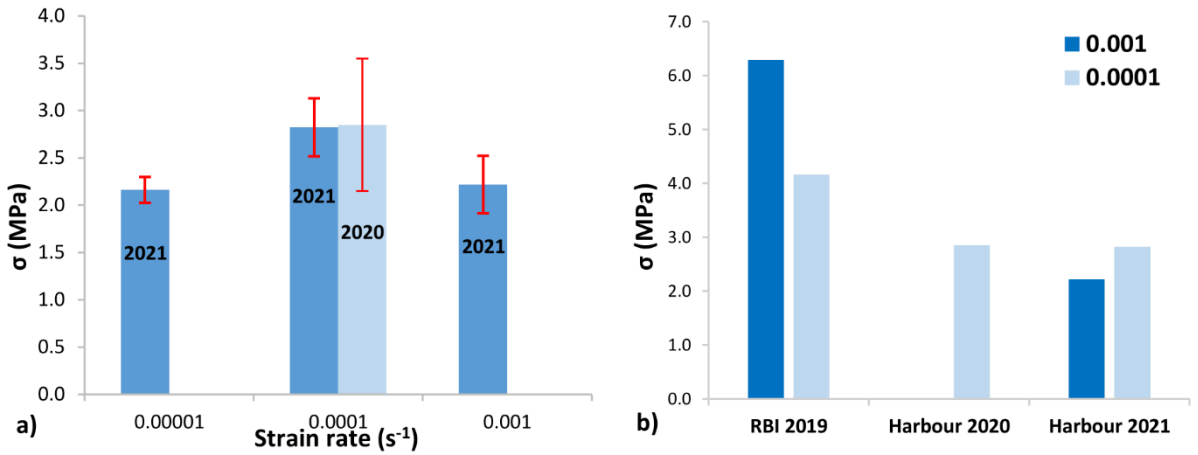

Figure 7. a) The average strength and the standard deviation of the brash ice samples vs strain

rates. The years 2020 and 2021 represent the brash ice pieces sampled from two different harbours. b) the horizontal uniaxial compressive strength of refrozen brash ice (RBI 2019) from a fully consolidated ship channel reported in the literature (Zhaka et al., 2020) is added for comparison.

4.3.1 Cyclic loading

Three cylinders sampled from brash ice pieces named P11, P12, and P13 were compressed with increasing strain rates of 10^{-5}, 10^{-4} and 10^{-3} s^{-1}. An example of the stress-strain curve obtained for P13 is given in Fig. 8a. The three maximum strength peaks for the three different strain rates can be clearly observed. The deformation of the cylinders due to compression increased the load that the sample could withstand when reloading for higher strain rates. Thus, the ice cylinders under cyclic loading exhibited strain-hardening behaviour. The maximum strengths obtained for all three samples and strain rates are given in Fig. 8b. Ice sample cored from P13 underwent the highest strength increase (almost doubled) when reloading the sample with higher strain rates. The kinematic hardening parameters of brash ice (from icebreaker- and Luleå harbours) under shear cyclic loading were discussed earlier by Patil et. al. (2022). It was found that the brash ice under shear exhibited kinematic hardening behaviour and became stronger with an increase in the confining axial force.

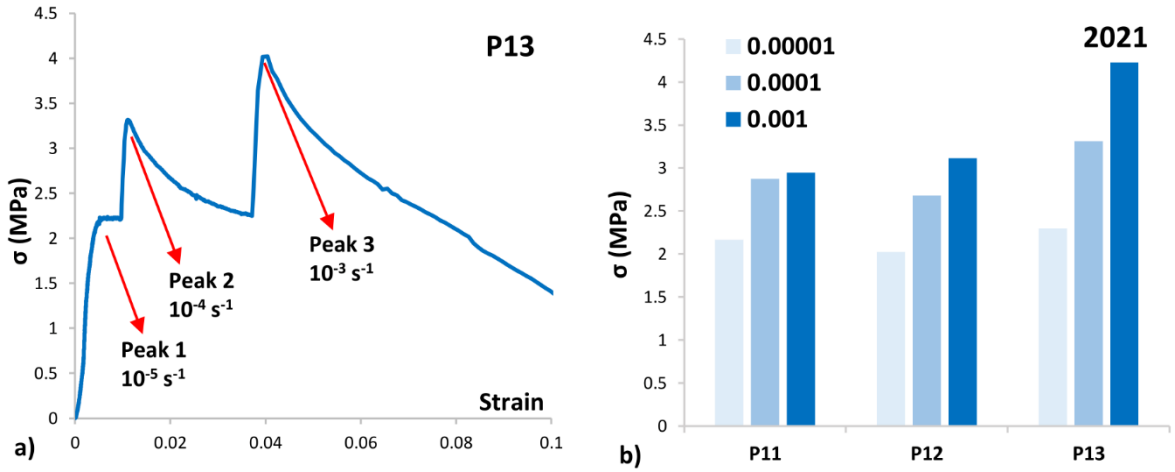

Figure 8. Example of stress-strain curve for the incremental strain increase for brash ice Piece 13 (a) and the maximum strength for all three pieces (b). In the first plot (a) the second force was applied about 20 minutes after the first one, but the third force was applied about 5 minutes after the second. The legend in the second plot (b) refers to the strain rate in units of s^{-1}.

CONCLUSIONS

Brash ice pieces were sampled from two different harbours in Luleå, Sweden, in March 2020 and March 2021. The first harbour was navigated by Swedish icebreakers (2020) while the second harbour was navigated by ice-breaking port tugs (2021). The first harbour was less frequently navigated, and the brash ice microstructure was similar to level ice, while the brash ice from the second harbour which was navigated on daily basis consisted of smaller and rounder ice pieces. The microstructure of these pieces was similar to that of deformed ice. A

three-parameter log-normal distribution function was found to represent the brash ice piece size distribution relatively well. The average compressive strength was not significantly different for the two harbours, but it was found to be half the strength of the refrozen brash ice sampled from a refrozen ship channel on the Finnish coast in 2019. The maximum compressive strength increased when the brash ice cylinders were exposed to cyclic loading under increasing strain rates from 10^{-5} s^{-1} to 10^{-3} s^{-1}.

ACKNOWLEDGEMENTS

The authors would like to acknowledge the support from TotalEnergies and Kolarctic ICEOP, and the help we received from the staff of Luleå harbour and the Swedish Maritime Administration. We would like to acknowledge the assistance received from Th. Forsberg. A special thanks to A. Patil for his contribution to planning the fieldwork and S. Pourzahedi for his assistance in the measurements.

REFERENCES

Bonath, V., Edeskär, T., Lintzén, N., Fransson, L., & Cwirzen, A., 2019a. Properties of Ice from First-Year Ridges in the Barents Sea and Fram Strait. *Cold Regions Science and Technology*, 168, 102890.

Bonath, V., Zhaka, V., Sand, B. 2019b. Field measurements on the behavior of brash ice. *In Proceedings of the 25th International Conference on Port and Ocean Engineering under Arctic Conditions, Delft, The Netherlands, 9–13 June.*

Boroojerdi, M. T., Bailey, E., & Taylor, R., 2020. Experimental study of the effect of submersion time on the strength development of freeze bonds. *Cold Regions Science and Technology*, 172, 102986.

Bridges, R., Riska, K., & Haase, A. 2019. Experimental tests on the consolidation of broken and brash ice. *In Proceedings of the 25th International Conference on Port and Ocean Engineering under Arctic Conditions, Delft, The Netherlands, 9–13 June.*

Eicken, H., 2003. From the microscopic, to the macroscopic, to the regional scale: growth, microstructure and properties of sea ice. Sea Ace: An Introduction to Its Physics, Chemistry, Biology and Geology, eds. Thomas, N. & Dieckmann, S. Chapter 2, pp. 22-81.

Ettema, R., & Huang, H. P. 1990. Ice formation in frequently transited navigation channels. *Cold Regions Research and Engineering Laboratory (CRREL), Special Report 90-40, 110 p.*

Fransson, L., Sand, B., Lundquist, J-E., Kärnä, T and Huffmeier, J., 2008. Ice Mechanics and Shipping in Ice-infested Waters. *Research report 2008:09, Luleå University of Technology, Sweden.*

Høyland, K. V., & Liferov, P., 2005. In the initial phase of consolidation. Cold Regions Science and Technology, 41(1), pp. 49-59.

Greisman. P., 1981. Brash ice behavior. U.S. *Coast Guard Research and Development Center*, Report No. USCG-D-30-81

Kitazawa, T., & Ettema, R., 1985. Resistance to ship-hull motion through brash ice. *Cold Regions Science and Technology,* 10(3), pp. 219–234.

Matala, R., Gong, H., 2021. The effect of ice fragment shape on model-scale brash ice material properties for ship model testing. *In Proceedings of the 26th International Conference on Port and Ocean Engineering under Arctic Conditions June, (pp. 14-18).*

Moslet, P. O., 2007. Field Testing of Uniaxial Compression Strength of Columnar Sea Ice. *Cold Regions Science and Technology*, 48(1), pp. 1–14.

Patil, A., Zhaka, V., Sand, B., Laue, J., & Cwirzen, A., 2022. Large-scale shear test of brash ice. *Ocean Engineering*, 249, 110935.

Sandkvist, J., 1982. Vertical block sizes in brash ice covered channels. *Forskningsrapport, Högskolan i Luleå 1 Jan 1974 → 31 Dec 1996).*

Sandkvist, J., 1986. Brash ice behaviour in frequented ship channels. *Water Resources Engineering, Luleå University of Technology, Luleå, Sweden*. Research Report Series A, No.139.

Shafrova, S., & Høyland K.V., 2008. Morphology and 2D Spatial Strength Distribution in Two Arctic First-Year Sea Ice Ridges. *Cold Regions Science and Technology*, 51(1), pp. 38–55.

Timco, G.W, & Frederking R.M.W., 1990. Compressive Strength of Sea Ice Sheets. *Cold Regions Science and Technology*, 17(3), pp. 227–240.

Zhaka, V., Bonath, V., Sand, B., & Cwirzen, A., 2020. Physical and mechanical properties of ice from a refrozen ship channel ice in the Bay of Bothnia. *In Proceedings of The 25th International Symposium on Ice*.